Interference Modeling of Cognitive Radio Networks

Xuemin Hong[†], Cheng-Xiang Wang[†], and John Thompson[††]

[†]Joint Research Institute for Signal and Image Processing, Heriot-Watt University, EH14 4AS, Edinburgh, UK.
[††]Joint Research Institute for Signal and Image Processing, University of Edinburgh, EH9 3JL, Edinburgh, UK.
Email: xh12@hw.ac.uk, cheng-xiang.wang@hw.ac.uk, john.thompson@ed.ac.uk

Abstract—**Cognitive radio (secondary) networks have been proposed as means to improve the spectrum utilization. A secondary network can reuse the spectrum of a primary network under the condition that the primary services are not harmfully interrupted. In this paper, we study the distribution of the interference power at a primary receiver when the interfering secondary terminals are distributed in a Poisson field. We assume that a secondary terminal is able to cease its transmission if it is within a distance of R to the primary receiver. We derive a general formula for the characteristic function of the random interference generated by such a secondary network. With this general formula we investigate the impacts of R, shadowing, and small scale fading on the probability density function (PDF) of the interference power. We find that when there is no interference region ($R = 0$), the interference PDFs follow heavy-tailed α-stable distributions. In case that a proper interference region is defined by a positive value of R, the tails of the interference power PDFs can be significantly shortened. Moreover, the impacts of shadowing and small scale fading on the interference PDFs are studied and the small scale fading is found to be beneficial in terms of reducing the mean value and outage probability of the interference power.**

I. INTRODUCTION

The radio spectrum is a scarce and precious nature resource. Traditionally, the whole spectrum is divided into smaller bands and each band is licensed for the exclusive use of one or several wireless applications. However, it has been shown that once time and space variations of spectrum occupation are taken into account, such a rigid spectrum licensing policy results in low spectrum utilization [1]. This imbalance between the spectrum scarcity and low utilization motivates the concept of cognitive radio (secondary) networks [2]–[4]. With the ability for each terminal to sense and adapt to the radio environment, a cognitive radio network can dynamically access the spectrum licensed to a primary network without compromising the incumbent primary service [5], [6].

In this paper, we are interested in the interference from secondary networks since it determines the degree to which the primary services are degraded by sharing spectrum with secondary networks. An accurate modeling of such interference is of great importance in designing a secondary network that can coexist well with primary networks. Simple *protocol models* [7]–[9] are frequently adopted in the literature as the interference model to study the capacities and protocols of cognitive radio networks. However, these models are widely considered as over-simplified. It is therefore desirable to have statistical interference models that provide detailed descriptions of the interference distribution.

For conventional (non-cognitive) radio networks, there is a wealth of literature regarding interference/noise modeling where the interferers are assumed to be distributed according to a Poisson point process in the plane [10]–[15]. It has been found that the interference PDF falls into the family of α-stable distributions, which are heavy-tailed. Such a heavy-tailed interference distribution is in general undesirable since it suggests a higher likelihood of disruptive interference.

Interference modeling of cognitive networks differs from that of conventional networks due to the distinct transmission characteristic of a cognitive terminal and a conventional terminal. While a conventional terminal transmits with a constant power, a cognitive terminal is able to optimize its transmission according to the radio environments. In this paper, we study one type of cognitive radio networks where a cognitive terminal is able to cease its transmission if it is within the "interference region" of any primary receiver. An interference region is defined as a disk centered at a primary receiver with a radius of R. Any cognitive terminal with this region is regarded as a harmful interferer and is therefore forbidden to transmit. In practice, a cognitive terminal can dynamically obtain the information about the interference region through either common signaling control channels [16] or primary receiver detection algorithms [17].

The interference generated by this type of cognitive radio networks has been studied in [18] where only the pathloss is considered for the propagation channels. When the radius of the interference region is sufficiently large, it was found that the interference at a primary receiver can be approximated by a confined Gaussian-like distribution – a much more desirable distribution for spectrum sharing systems compared with a heavy-tailed α-stable distribution. In this paper, we extend the analysis in [18] to take into account the shadowing and fading effects of the channels. Through numerical studies we find that shadowing and fading change the shape of the PDFs of the interference by prolonging the tails. Therefore, a Gaussian approximation is no longer valid and the PDFs of the interferences seem to be better approximated by log-normal distributions.

The remainder of this paper is organized as follows. Section II describes the system model. In Section III, we study the distribution of the interference from cognitive transmitters. Numerical results are presented in Section IV followed by discussions. Finally, conclusions are drawn in Section V.

II. SYSTEM MODEL

The system model is shown in Fig. 1. We consider a primary receiver (Rx) with an omnidirectional antenna. We also assume an ideal infinite secondary network with an infinite number of secondary transmitters (Txs). The location of secondary terminals in the plane follows a Poisson point process with a density parameter λ_a, which denotes the average number of secondary terminals per unit area. We assume that the probability of a terminal on transmission is p. The set of transmitting terminals also forms a Poisson process with density parameter $\lambda = p\lambda_a$. The primary receiver has an "interference region" given by a disk centered at the primary receiver with a radius of R. Any secondary device located within the interference region is not allowed to transmit. On the other hand, all other active secondary terminals outside this interference region can transmit with power P_j, where j $(1 \leq j < \infty)$ is the index for active secondary terminals. It is worth noting that the interference region here is defined by primary receivers rather than primary transmitters. When power control is applied in the secondary network, we may consider $\{P_j\}$ as independent random variables with identical distributions. The distance between the jth active secondary transmitter and the primary receiver is denoted as r_j, where $R \leq r_1 \leq r_2 \leq \ldots \leq r_\infty$. The channel gain between the jth secondary transmitter and the primary receiver can be expressed as the product of two factors: the pathloss and composite shadowing and fading. Let $g(r)$ denote the pathloss power gain at a distance r from the transmitter of the signal. The exact form of $g(r)$ will depend on the environment. For a general discussion and mathematical convenience, we follow [10] and assume that $g(r)$ is a monotonically decreasing function which satisfies $\lim_{r \to 0} g(r) = \infty$ and $\lim_{r \to \infty} g(r) = 0$. Furthermore, let h_j denote the normalized composite shadowing and fading random variable with unit mean. We assume that the random variables $\{h_j\}$ are mutually independent and have identical PDFs, denoted as $f_h(x)$. When lognormal shadowing and Nakagami fading are assumed, $f_h(x)$ can be approximated by a log-normal distribution as [19]

$$f_h(x) \approx \frac{10}{\ln 10 \sqrt{2\pi}\sigma x} \exp\left\{-\frac{(10\log_{10} x - \mu)^2}{2\sigma^2}\right\}. \quad (1)$$

In (1), the mean μ and variance σ^2 are given by [19]

$$\mu = \epsilon^{-1}\left[\psi(m) - \ln(m)\right] \quad (2)$$

$$\sigma^2 = \epsilon^{-2}\zeta(2, m) + \sigma_s^2 \quad (3)$$

respectively, where $\epsilon = \ln(10)/10$ is a constant, m is the Nakagami shaping factor, σ_s is the standard deviation of the lognormal shadowing, $\psi(\cdot)$ is the Euler psi function, and $\zeta(\cdot, \cdot)$ is Riemann's zeta function [19]. The power of the interference perceived at the primary receiver is then given by

$$Y = \sum_{j=1}^{\infty} g(r_j)x_j. \quad (4)$$

where $x_j = P_j h_j$. Clearly, $\{x_j\}$ are mutually independent and have identical distributions, denoted as $f_X(x)$. The random variable that has a distribution of $f_X(x)$ is denoted as X and we have $0 \leq X < \infty$.

III. INTERFERENCE MODELING

In this section, we wish to find the probability density function (PDF) of Y given by (4). The approach used in [10] for interference modeling of multihop networks is adopted here and generalized for the above described system model. Let Y_l be the total interference power received from those active secondary transmitters which are in a disk of radius l, i.e.,

$$Y_l = \sum_{R \leq r_j \leq l} g(r_j)x_j. \quad (5)$$

Subsequently, we will first work on the characteristic function of Y_l. The characteristic function of Y can then be obtained with $l \to \infty$. The PDF of Y is then the inverse Fourier transform of its characteristic function. By definition, the characteristic function of Y_l is given by

$$\phi_{Y_l}(\omega) = E(e^{i\omega Y_l}) \quad (6)$$

where $E(\cdot)$ is the expectation operator. The calculation of the expectation in (6) can be broken down into two steps using conditional expectations. The inner expectation is taken over Y_l given that there are k active secondary transmitters within the disk of radius l, followed by an outer expectation taken over k, i.e., [10]

$$
\begin{aligned}
\phi_{Y_l}(\omega) &= E(E(e^{i\omega Y_l}|k)) \\
&= \sum_{k=0}^{\infty} \frac{e^{-\lambda\pi D_l}(\lambda\pi D_l)^k}{k!} E(e^{i\omega Y_l}|k) \quad (7)
\end{aligned}
$$

where $D_l = l^2 - R^2$. According to the nature of the Poisson process, given that there are k terminals in the area of πD_l, $\{r_j\}$ have identical uniform distributions [10]. Let V denote the random variable with the same uniform distribution, it follows that the PDF of V is given by

$$f_V(r) = \begin{cases} 2r/D_l & R \leq r \leq l \\ 0 & \text{otherwise.} \end{cases} \quad (8)$$

Since Y_l is the sum of a number of independent random variables, the conditional expectation $E(e^{i\omega Y_l}|k)$ denoting the characteristic function of Y_l given k can then be written as the product of individual characteristic functions, i.e.,

$$E(e^{i\omega Y_l}|k) = [E(e^{i\omega g(V)X})]^k. \quad (9)$$

Substituting (8) and (9) into (7), we have

$$\phi_{Y_l}(\omega) = e^{\lambda\pi D_l(Q-1)} \quad (10)$$

where

$$
\begin{aligned}
Q &= E(e^{i\omega g(V)X}) \\
&= \int_x f_X(x) \int_R^l e^{i\omega g(r)x} \frac{2r}{D_l} dr dx. \quad (11)
\end{aligned}
$$

Taking the integral over r and considering $l \to \infty$ we get

$$Q = 1 + \frac{1}{D_l}\int_x f_X(x)T(\omega x)dx \quad (12)$$

1852

where

$$T(\omega x) = R^2(1 - e^{i\omega g(R)x}) + i\omega x \int_0^{g(R)} [g^{-1}(t)]^2 e^{i\omega tx} dt. \tag{13}$$

Note that in (13), $g^{-1}(\cdot)$ denotes the inverse function of $g(\cdot)$. Substituting (12) into (10), with $l \to \infty$ we obtain

$$\phi_Y(\omega) = \exp\left(\lambda\pi \int_x f_X(x)T(\omega x)dx\right). \tag{14}$$

Equation (14) serves as a general formula to calculate the characteristic function of Y. Taking its inverse Fourier transform results in the PDF $f_Y(y)$ of Y, i.e.,

$$f_Y(y) = \frac{1}{2\pi} \int_{-\infty}^{\infty} e^{-i\omega y}\phi_Y(\omega)d\omega. \tag{15}$$

It is difficult to simplify (12) further except for some special scenarios. To proceed further, we may first specify $g(r) = 1/r^\beta$, where β is the pathloss exponent.

A. Secondary Networks Without Interference Region

For secondary networks without any interference region, we have $R = 0$ and consequently $g(R) \to \infty$. With a typical value of the pathloss exponent $\beta = 4$, following similar steps in [10] we can obtain the closed-form expression of the PDF of Y as

$$f_Y(y) = \frac{\pi}{2}K\lambda y^{-3/2}\exp\left(-\frac{\pi^3\lambda^2 K^2}{4y}\right) \tag{16}$$

where

$$K = \int_x f_X(x)\sqrt{x}dx. \tag{17}$$

The above PDF falls into the category of Levy distribution $S_{1/2}(\sigma, 1, \mu)$ [20], [21] with the scale parameter $\sigma = \pi^3\lambda^2 K^2/2$ and the shift parameter $\mu = 0$.

B. Mean Interference Distribution

Previously in (4) , we have modeled $\{x_j\}$ as random variables to account for the power control and channel fading. Therefore, Y given by (4) represents the instantaneous interference power and would have impact on the instantaneous signal-to-interference-and-noise ratio (SINR) at the primary receiver. However, in some applications, e.g., delay-insensitive services, the quality of service (QoS) of the primary network is determined by the average SINR [22]. In this case, we are interested in the mean interference power, i.e., the power averaged over fading and power control states. It follows that (4) becomes

$$Y = \Omega \sum g(r_j) \tag{18}$$

where $\Omega = E(x_j) = E(P_j)E(h_j)$ can be treated as a constant and therefore only has a scaling effect on Y. Without loss of generality we assume $\Omega = 1$. The characteristic function of Y in this special case can be obtained by treating X as a constant in the general framework discussed previously. It is easy to show that the characteristic function is given by

$$\phi_Y(\omega) = \exp(\lambda\pi T(\omega)) \tag{19}$$

where

$$T(\omega) = R^2(1 - e^{i\omega g(R)}) + i\omega \int_0^{g(R)} [g^{-1}(t)]^2 e^{i\omega t} dt. \tag{20}$$

IV. NUMERICAL RESULTS AND DISCUSSIONS

In this section, we will evaluate the PDF of Y numerically. First of all, Fig. 2 shows the Levy distribution based on (16) with different values of $K\lambda$. As discussed previously, it represents the interference power distribution of a secondary network without any interference region. The Levy distributions are featured by their heavy-tailed PDFs. This is an undesirable feature in the context of cognitive radio networks since it means that it is more difficult to predict and control the interference caused by secondary networks.

Figs. 3 and 4 are obtained by numerically evaluating the inverse Fourier transform of $\phi_Y(\omega)$ given in (19). They represent the interference power distributions of a cognitive network with a interference region, where the interference power is averaged over power control and channel fading states. Fig. 3 is obtained with $\lambda = 1$ and different values of R. A larger value of R means a wider area of interference region so that the primary receiver is better protected. As we can see from Fig. 3, both the mean value and variance of the interference power decrease with the increasing R. The case of $R = 0$ leads to a heavy-tailed Levy distribution shown previously in Fig. 2. With non-zero values of R, the tails are shortened and the distribution of the interference power tends to be more confined. Interestingly, when the value of R is large enough, the distribution looks very similar to a Gaussian distribution. Fig. 3 provides an insight that the heavy-tailed distribution observed in Fig. 2 is due to the small number of dominant interferers nearby the victim receiver. Once these nearby interferers are eliminated, there will be no dominant interferers and all the rest interferers would contribute a small portion to the total interference power. Consequently, the central limit theorem can be applied and the total interference power tends to be Gaussian distributed.

In Fig. 4, we assume $R = 1$ m and show the impacts of the terminal density λ and average transmit power Ω on the interference power distribution. As expected, Gaussian-like distributions are observed. Moreover, with the increasing λ, the mean of the interference power scales linearly with λ, whereas the variance increases slower than a linear scale. On the other hand, as discussed in Sub-section III.B, the average transmit power Ω has a scaling effect on the interference Y. When Y follows a Gaussian distribution, both the mean and variance would be scaled by Ω to the same degree. The difference of the scaling effects of λ and Ω can be seen by comparing the two distributions obtained with ($\lambda = 2$, $\Omega = 1$) and ($\lambda = 1$, $\Omega = 2$), both scaled from that with ($\lambda = 1$, $\Omega = 1$). The two distribution curves have roughly the same mean but a smaller variance is observed for the former case. This means that in terms of interference outage probability, doubling the density of the secondary terminals would be less disruptive to the primary network than doubling the average transmission power of the secondary terminals.

In Fig. 5, we evaluate the instantaneous interference power whose characteristic function is given by (14). We assume that the secondary terminals transmit with constant powers and the channels are subject to log-normal shadowing and Nakagami fading as described in Section II. We assume that the standard deviation of the the log-normal shadowing $\sigma_s = 8$ dB and the Nakagami shaping factor $m = 1$, which corresponds to the case of Rayleigh fading. Using the same sets of parameters of Fig. 3, the PDFs of instantaneous interference power are shown in Fig. 5. We can see that the PDFs in Fig. 5 has slightly heavier tails than that in Fig. 3. This is because that when the effects of fading and shadowing are taken into account, there is a higher probability that a strong and dominant interference would occur, which violates the applicability of the central limit theorem and results in a non-Gaussian distribution with heavier tails.

The PDFs of the instantaneous interference power are shown in Fig. 6 with different values of the Nakagami shaping factor m to show the impacts of small scale fading on the interference distribution. The standard deviation of the lognormal shadowing is taken to be $\sigma_s = 8$ dB. When $m = 1$ we have a composite Rayleigh-log-normal fading channel whereas when $m = 1000$ the channel is dominated by log-normal shadowing. Interestingly, from Fig. 6 we can see that the interference power given by $m = 1$ has a smaller mean and better outage property compared with that given by $m = 1000$. In other words, severe fading can be beneficial in terms of reducing the interference from secondary networks to primary networks. Finally, from Fig. 5 and Fig. 6 we can see that the PDF of the interference power can no longer be approximated by a Gaussian distribution. An approximation with a lognormal distribution seems to be more appropriate, the detail of which is for future work.

V. CONCLUSIONS

In this paper, we have studied the distribution of the interference generated by a secondary network to a primary network. The secondary terminals are assumed to be cognitive so that they can cease the transmission if any primary receiver within a distance of R is detected. We have studied the characteristic function of the random interference and derived a general formula taking into account the cognitive ability, power control, and channel fading. Under the same framework, two special cases, namely, the interference PDFs in a cognitive network without interference region and the mean interference PDFs averaged over shadowing and fading states, have been further investigated. Numerical results have shown that with a predefined interference region, a cognitive secondary network achieves much smaller interference outage probability than a secondary network without any interference region. Moreover, the PDFs of the instantaneous interference power have heavier tails than the PDFs of the mean interference power averaged over shadowing and fading states. Finally, small scale fading are shown to have effects on reducing the mean and variance of the instantaneous interference power.

REFERENCES

[1] Federal Communication Commission, Spectrum policy task force report, Washington DC, FCC 02-155, 2 Nov. 2002.
[2] J. Mitola and G. Maguire, "Cognitive radio: making software radios more personal", *IEEE Personal Commun. Mag.*, vol. 6, no. 6, pp. 13–18, Aug. 1999.
[3] S. Haykin, "Cognitive radio: brain-empowered wireless communications", *IEEE J. Select. Areas Commun.*, vol. 3, no. 2, pp. 201–220, Feb. 2005.
[4] H. H. Chen and M. Guizani, *Next Generation Wireless Systems and Networks*, Chichester: John Wiley & Sons, 2006.
[5] Federal Communications Commission, Unlicensed operation in the TV broadcast bands, ET Docket No. 04-186, 2004.
[6] Federal Communication Commission, Facilitating opportunities for flexible, efficient, and reliable spectrum use employing cognitive radio technologies, NPRM & Order, ET Docket No. 03-108, FCC 03-322, 30 Dec. 2003.
[7] T. X. Brown, "An analysis of unlicensed device operation in licensed broadcast service bands", *Proc. IEEE DySPAN'05*, Baltimore, USA, Nov. 2005, pp. 11-29.
[8] S. A. Jafar and S. Srinivasa, "Capacity limits of cognitive radio with distributed and dynamic spectral activity," *Proc. IEEE ICC'06*, Istanbul, Turkey, June 2006, pp. 5742–5747.
[9] J. Bater, H.-P. Tan, K. N. Brown, and L. Doyle, "Modelling interference temperature constraints for spectrum access in cognitive radio networks," *Proc. IEEE ICC'07*, Glasgow, UK, June 2007, pp. 6493–6498.
[10] E. S. Sousa and J. A. Silvester, "Optimum transmission range in a direct-sequence spread-spectrum multihop pack radio network," *IEEE J. Sel. Area Commun.*, vol. 8, no. 5, pp 762-771, June 1990.
[11] E. S. Sousa, "Performance of a spread spectrum packet radio network link in a poisson field of interferers," *IEEE Trans. Infor. Theory*, vol. 38, no. 6, pp. 1743-1754, Nov. 1992.
[12] J. Ilow and D. Hatzinakos, "Analytic alpha-stable noise modelling in a poisson field of interferers or scatterers," *IEEE Trans. Signal Processing*, vol. 46, no. 6, pp. 1601-1611, June 1998.
[13] X. Yang and A. P. Pertropulu, "Co-channel interference modeling and analysis in a Poisson field of interferers in wireless communications," *IEEE Trans. Signal Processing*, vol. 51, no. 1, pp. 63-76, Jan 2003.
[14] P. C. Pedro, C.-C. Chong, A. Giorgetti, M. Chiani, and M. Z. Win, "Narrowband Communication in a Poisson Field of Ultrawideband Interferers," *Proc. IEEE ICUWB'06*, Boston, USA, Sept. 2006, pp. 387–392.
[15] P. C. Pinto and M. Z. Win, "Communication in a poisson field of interferers," *Proc. IEEE 40th Annual Conf. Inform. Sciences and Systems*, Princeton, NJ, USA, Mar. 2006, pp. 432–437.
[16] S. Mangold, A. Jarosch, and C. Monney, "Operator assisted cognitive radio and dynamic spectrum assignment with dual beacons – detailed evaluation," *Proc. First Intl. Conf. on Commun. Systems Software and Middleware*, Jan. 2006, pp. 1–6.
[17] B. Wild and K. Ramchandran, "Detecting primary receivers for cognitive radio applications", *Proc. IEEE DySPAN'05*, Baltimore, USA, Nov. 2005, pp. 124-130.
[18] R. Menon, R.M. Buehrer, and J.H. Reed, "Outage probability based comparison of underlay and overlay spectrum sharing techniques", *Proc. IEEE DySPAN'05*, Baltimore, USA, Nov. 2005, pp. 101–109.
[19] G. L. Stuber, *Principles of Mobile Communication*, 2nd Edition, Boston: Kluwer Academic Publishers, 2001.
[20] A. Janicki and A. Aweron, *Simulation and Chaotic Behaviour of α-stable Stochastic Processes*, New York: Marcel Dekker, 1994.
[21] G. Samorodnitsky and M. S. Taqqu, *Stable Non-Gaussian Random Processes*, New York: Chapman & Hall, , 1994.
[22] A. Ghasemi, and E. S. Sousa, "Capacity of fading channels under spectrum-sharing constraints," *Proc. IEEE ICC'06*, Istanbul, Turkey, June 2006, pp. 4373–4378.
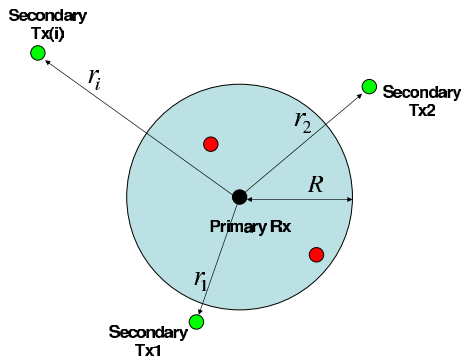
Fig. 1. System model: secondary transmitters distributed in a Poisson filed and a primary receiver with an interference region of radius R.
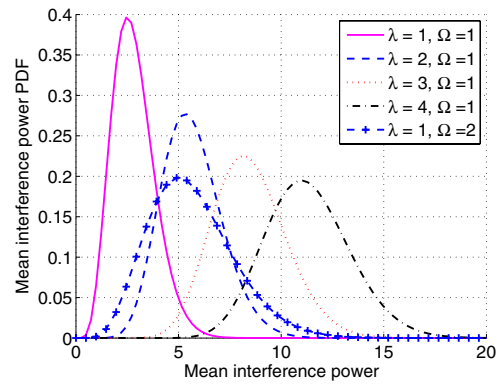
Fig. 4. Mean interference power PDFs with an interference region ($R = 1$ m).
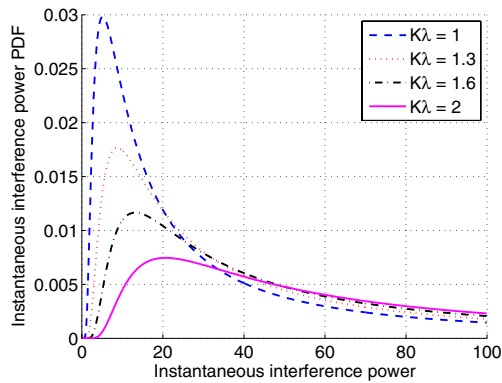
Fig. 2. Mean interference power PDFs without interference region ($R = 0$).
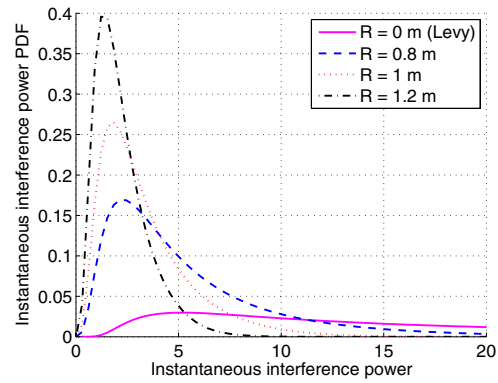
Fig. 5. Instantaneous interference power PDFs with an interference region ($\lambda = 1$, $\sigma_s = 8$ dB, and $m = 1$).
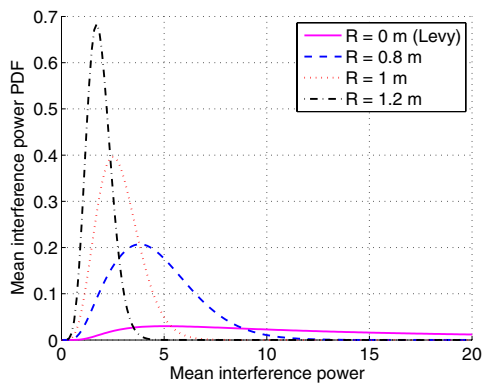
Fig. 3. Mean interference power PDFs with an interference region ($\Omega = 1$ and $\lambda = 1$).
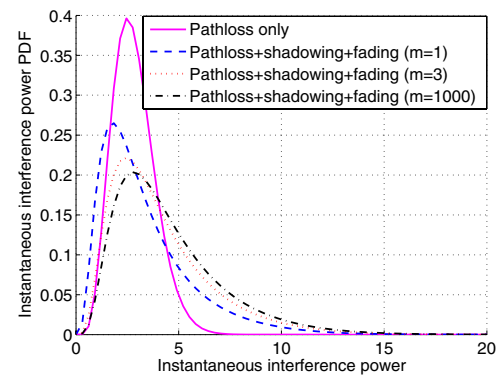
Fig. 6. Instantaneous interference power PDFs with an interference region under different fading scenarios ($R = 1$ m, $\lambda = 1$, and $\sigma_s = 8$ dB).

1855